Multi-Look Stripmap SAR Processing with Built-In Geometric Correction

Oleksandr O. Bezvesilniy, Ievgen M. Gorovyi, Sergiy V. Sosnytskiy, Volodymyr V. Vynogradov, Dmytro M. Vavriv
Institute of Radio Astronomy of NAS of Ukraine
Kharkov, Ukraine
vavriv@rian.kharkov.ua

Abstract—**Small airborne SAR systems suffer from trajectory deviations and instabilities of antenna orientation. These kinds of motion errors lead to significant geometric distortions in SAR images. In the paper, we describe a time-domain multi-look stripmap SAR processing algorithm with built-in geometric correction. In the algorithm, the azimuth reference functions and range migration curves are designed to produce SAR images directly on a correct rectangular grid on the ground plane. The proposed technique has been successfully tested by using a Ku-band airborne SAR system, installed on a light-weight aircraft.**

Keywords-synthetic aperture radar; airborne SAR; geometric distortions;multi-look processing

I. Introduction

Forming high-quality multi-look SAR images with airborne SAR systems installed on small aircrafts is a difficult problem because of significant motion and orientation errors of such light-weight platforms. Deviations of the aircraft trajectory and instabilities of the antenna orientation lead to geometric and radiometric errors in SAR images [1-3].

Geometric distortions of SAR images could be corrected by interpolation of images to a rectangular grid on the ground plane taking into account the measured aircraft trajectory and the orientation of the synthetic aperture beams (SAR beams). However, this approach could be inefficient in case of significant geometric distortions.

The commonly-used clutter-lock technique [4], which is based on the estimation of the Doppler centroid from radar data, helps prevent radiometric errors very effectively in case of uncertain but stable antenna orientation. However, the clutter-lock should not be used in case of fast and significant instabilities of the antenna orientation since it leads to strong geometric errors in SAR images.

Instabilities of the aircraft orientation could be compensated by the antenna stabilization. However, it is a complicated and expensive solution. An application of a wide-beam antenna firmly mounted on the aircraft is another way to guarantee the uniform illumination of the ground scene despite of the instabilities of the platform orientation.

In the paper, we describe a time-domain multi-look stripmap SAR processing algorithm with built-in correction of geometric distortions. In the algorithm, the azimuth reference functions and range migration curves are specially designed to produce SAR images directly on a correct rectangular grid on the ground plane.

The proposed approach does not use the clutter-lock – the orientation of the SAR beams is fixed. Therefore, the algorithm works well without an additional radiometric correction only for a wide-beam antenna and for SAR looks which are close to the centre of the antenna beam. In order to track the illuminated spot and produce a multi-look SAR image composed of all available SAR looks, we have proposed an effective radiometric correction technique based on by multi-look processing with extended number of looks [7].

The proposed techniques have been successfully tested by using a Ku-band airborne SAR system, installed on a light-weight aircraft [5].

II. Time-Domain Convolution-Based SAR Processing

In order to form the synthetic aperture, the received pulses should be summed up coherently taking into account the propagation phase $\varphi(\tau) = -4\pi R(\tau)/\lambda$, where $R(\tau)$ is the slant range to the target, λ is the radar wavelength. The formation of the synthetic aperture $I(t)$ is performed by convolving the received signal $s(t)$ with the reference function $h(\tau)$:

$$I(t) = \left| \frac{1}{T_S} \int_{-T_S/2}^{T_S/2} s(t+\tau) h(\tau) d\tau \right|^2 , \quad (1)$$

$$h(\tau) = w(\tau) \exp\left[i \frac{4\pi}{\lambda} R(\tau) \right]. \quad (2)$$

The weighting window $w(\tau)$ is applied to improve the side-lobe level of the synthetic aperture pattern.

If the slant range $R(\tau)$ to the target changes during the time of synthesis T_S more than the size of the range resolution cell then the target signal “migrates” through several range cells. This effect known as range migration should be taken into account during the aperture synthesis. The onedimensional backscattered signal $s(t)$, which is convolved with the reference function in (1), should be obtained from the two-dimensional «azimuth – slant range» matrix of the received signals by interpolation along the migration curve:

$$R(\tau) \approx R - \frac{\lambda}{2} F_{DC} \tau - \frac{\lambda}{2} F_{DR} \frac{\tau^2}{2} . \qquad (3)$$

The Doppler centroid F_{DC} and the Doppler rate F_{DR} are given by

$$F_{DC} = \frac{2}{\lambda} \frac{(\vec{\mathbf{R}} \cdot \vec{\mathbf{V}})}{R} , \qquad (4)$$

$$F_{DR} = -\frac{2}{\lambda} \left[\frac{V^2}{R} \left(1 - \frac{(\vec{\mathbf{R}} \cdot \vec{\mathbf{V}})^2}{R^2 V^2} \right) - \frac{(\vec{\mathbf{R}} \cdot \vec{\mathbf{A}})}{R} \right] . \qquad (5)$$

Here $\vec{\mathbf{V}}$ and $\vec{\mathbf{A}}$ are the aircraft velocity and acceleration vectors, correspondingly. The slant range vector $\vec{\mathbf{R}}$ goes from the antenna phase center to the point (x_R, y_R) on the ground at which the synthetic beam will be aimed (see Fig. 1). The point (x_R, y_R) is on the Doppler centroid line AB which is the intersection of the elevation plane of the real antenna pattern and the ground plane. In this case the SAR beam will be pointed at the center of the real antenna beam. The x-axis of the local coordinate system is always pointed along the horizontal component of the aircraft velocity vector (so that $V_y = 0$). The z-axis is pointed upward and goes through the antenna phase center, H is the aircraft flight altitude. The orientation of the real antenna is described by the antenna pitch angle α and the antenna yaw angle β so that

$$x_R = H \tan\alpha \cos\beta + \sin\beta \sqrt{R^2 - (H / \cos\alpha)^2} , \qquad (6)$$

$$y_R = -H \tan\alpha \sin\beta + \cos\beta \sqrt{R^2 - (H / \cos\alpha)^2} . \qquad (7)$$

The aircraft flight altitude, velocity and acceleration, as well as the antenna beam orientation angles may change slowly but they are assumed to be constant during the time of synthesis.

The azimuth resolution is given by

$$\rho_X = K_w \frac{V_X}{|F_{DR}| T_S} , \qquad (8)$$

The coefficient K_w describes broadening of the main lobe of the synthetic aperture pattern caused by windowing.

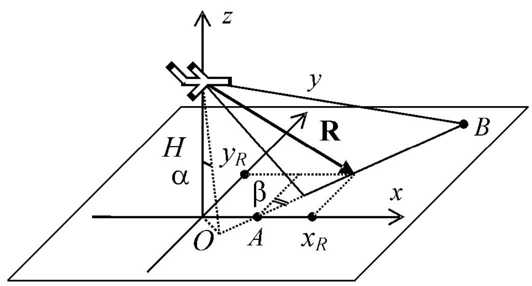

Figure 1. Stripmap SAR geometry.

The method of the formation of the synthetic aperture following (1)-(3) is known as the time-domain convolution-based SAR processing algorithm with range migration correction by interpolation. The algorithm is effective for building moderate-resolution SAR images when the convolution is not too long.

The advantage of the algorithm is its ability to build each pixel of the SAR image with a particular reference function and migration curve. It means that the algorithm works well for time-varying and range-dependent Doppler centroid and Doppler rate, which is the case of small aircraft SAR systems.

III. Time-Domain Multi-Look SAR Processing

In the stripmap mode, the best (the highest) azimuth resolution is limited by the real antenna beam width and is approximately equal to the half of the antenna azimuth length. SAR systems are often equipped with small, compact antennas and the best azimuth resolution may be much higher than the required azimuth resolution, which is typically chosen to be equal to the range resolution. In this case, the multi-look SAR processing technique can be effectively used to form multiple synthetic beams and obtain several SAR images (looks) of the same scene [1, 6]. The non-coherent summation (averaging) of SAR looks is used to suppress speckle noise in SAR images.

For multi-look processing, the whole azimuth Doppler bandwidth

$$\Delta F_{D\max} = F_{DR} T_{S\max} , \qquad (9)$$

is divided on the sub-bands which may partly overlap. For half-overlapped sub-bands the central frequencies and width of the sub-bands of the SAR looks are

$$F_{DC}(n_L) = F_{DC}(R) + \Delta F_{DC}(n_L) , \qquad (10)$$

$$\Delta F_{DC}(n_L) = n_L \frac{\Delta F_D(N_L)}{2} , \qquad (11)$$

$$\Delta F_D(N_L) = 2 \Delta F_{D\max} / (N_L + 1) , \qquad (12)$$

where $n_L = -N_L / 2, ..., N_L / 2 - 1$.

The Doppler bandwidth of the SAR look corresponds to the time of synthesis:

$$T_{SL} = 2T_{S\max} /(N_L + 1)\,. \qquad (13)$$

Taking into account the relation (8) for the azimuth resolution, the central frequencies of the SAR looks (11) can be written as

$$F_{DC}(R) + \Delta F_{DC}(n_L) = F_{DC}(R) - n_L \frac{K_w}{2}\frac{V_X}{\rho_X}\,. \qquad (14)$$

The multi-look processing could be based on dividing of the reference function built on the whole long interval of synthesis $T_{S\max}$ on several sub-intervals. In this first approach we should guarantee that there are no significant uncompensated phase errors during this long coherent processing time. However, as a matter of fact, in order to achieve the desired azimuth resolution for one SAR look it is sufficient to perform coherent processing on the shorter time interval T_{SL} (13). According to this second approach, which is much preferable in case of significant motion errors, we should process the data collected during the time of synthesis T_{SL} with a set of different reference functions to form multi-look SAR beams. The question is how to build the reference functions.

As it has been shown in the previous section, in order to aim the SAR beam at the point (x_R, y_R) we should perform processing with the corresponding range migration curve (3), the Doppler centroid $F_{DC}(R)$ (4), and the Doppler rate $F_{DC}(R)$ (5). The SAR look beam formed with the central frequency $F_{DC}(R) + \Delta F_{DC}(n_L)$ will be pointed to some point $(x_R + \xi_n, y_R + \eta_n)$. What are the coordinates of this point?

First, since the signal from this point has appeared at the slant range R when the aircraft is at the center of the synthetic aperture, we can write:

$$\sqrt{x_R^2 + y_R^2 + H^2} = \sqrt{(x_R + \xi_n)^2 + (y_R + \eta_n)^2 + H^2}\,,$$

$$x_R^2 + y_R^2 = (x_R + \xi_n)^2 + (y_R + \eta_n)^2\,. \qquad (15)$$

Second, the position of the point in azimuth direction is related to its Doppler centroid (4), so we can write:

$$F_{DC}(R) + \Delta F_{DC}(n) = \frac{2}{\lambda}\frac{(x_R + \xi_n)V_X - HV_Z}{R}\,,$$

$$\Delta F_{DC}(n) = \frac{2}{\lambda}\frac{V_X}{R}\xi_n\,. \qquad (16)$$

Thus, in order to form the set of SAR looks for slant range R with central frequencies (14) we should first calculate the corresponding points $(x_R + \xi_n, y_R + \eta_n)$ on the ground from (15) and (16) and then process the same raw data on the interval of synthesis T_{SL} with the appropriate range migration curves (3), Doppler centroids (4) and Doppler rates (5).

It should be noted that SAR look beams are aimed at different points on the ground. It means that SAR look images are sampled on different grids. Therefore, SAR look images should be first re-sampled to the same ground grid and only then they can be averaged to produce the multi-look image. The deviations of the aircraft trajectory introduce further complexity into the re-sampling process. An efficient approach to solve this problem called "built-in correction of geometric distortions" is proposed in the next section.

IV. BUILT-IN CORRECTION OF GEOMETRIC DISTORTIONS

The idea of built-in correction of geometric distortions is to point the multi-look SAR beams exactly to the nodes of the rectangular grid on the ground plane. In this way, we immediately obtain geometrically correct SAR look images. This approach cannot be combined with the clutter-lock and radiometric errors could appear in case of fast and considerable instabilities of the antenna orientation, especially for narrow-beam antenna. An effective radiometric correction procedure is proposed in [7].

The built-in geometric correction consists of the following steps. First, we should specify the reference flight trajectory with the constant aircraft flight altitude H_0, velocity V_0, and the pulse repetition period T_0, as well as the reference orientation of the antenna beam with the constant antenna pitch and yaw angles α_0 and β_0. These reference parameters are used to calculate the time-independent Doppler centroid $F_{DC}(R)$ and the central Doppler frequencies of SAR looks $F_{DC}(R) + \Delta F_{DC}(n_L)$, and coordinates of the reference points on the ground plane, to which the SAR look beams should be pointed:

$$x_{ref}(n_L, R)\,,\; y_{ref}(n_L, R)\,. \qquad (17)$$

After that we should find the nodes of the correct rectangular grid on the ground, which are close to these points, (by using interpolation):

$$x_{ref}^{node}(n_L, i_Y)\,,\; y_{ref}^{node}(n_L, i_Y)\,. \qquad (18)$$

Here i_Y is the in ground range index of the grid.

There are two important requirements for the azimuth grid step Δx. First, the grid step must be multiple of the pulse repetition path:

$$\Delta x = \Delta y = k_\Delta V_0 T_0\,. \qquad (19)$$

where k_Δ is an integer number. Second, there must be at least one sample per resolution cell:

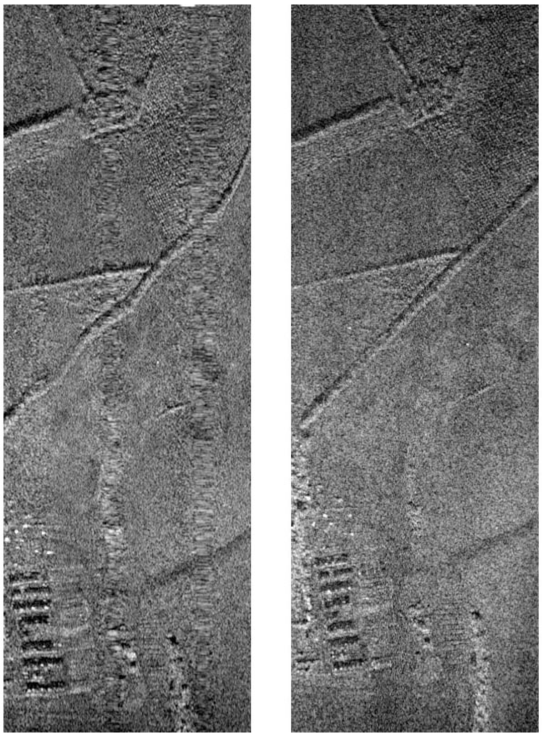

Figure 2. The left SAR image is built by using clutter-lock. The right SAR image is formed by using the built-in geometric correction.

Figure 3. SAR image (45 looks) formed by using the built-in geometric correction is imposed on the Google Map image.

$$\Delta x = \Delta y = \rho_x / k_s , \ k_s \geq 1 . \quad (20)$$

Typically, the sampling factor is chosen to be $k_s \approx 2$ (two samples per resolution cell). If the coordinates of the nodes of the adjacent looks $x_{ref}^{node}(n_L, i_Y)$ and $x_{ref}^{node}(n_L+1, i_Y)$ are closer than the grid step Δx, these nodes will coincide. To prevent such situation we should decrease the grid step Δx and, consequently, increase the sampling factor k_s.

Finally, in order to produce geometrically correct SAR images we should point the synthetic beams to the corresponding nodes:

$$x_{ref}^{node}(n_L, i_Y) + i_X \Delta x , \ y_{ref}^{node}(n_L, i_Y) . \quad (21)$$

To do this, we should transform the coordinates of these nodes from the reference local coordinate system to the actual local coordinate system taking into account actual aircraft position and orientation of the velocity vector. Thus, we obtain SAR image samples $SAR(n_L, i_X, i_Y)$ in the nodes (i_X, i_Y) of the rectangular grid of the ground plane.

V. Results

The geometric correction is illustrated in Fig. 2. The left SAR image is built by using clutter-lock. One can see geometric distortions caused by instabilities of the antenna orientation. The right SAR image is formed by using the algorithm with the built-in geometric correction. Both images have 3-m resolution and are built using 3 looks.

The accuracy of the geometric correction is illustrated in Fig. 3, where the SAR image composed of 45 looks and formed by using the built-in geometric correction is imposed on the Google Map image of the scene. One can see that the multi-look SAR processing algorithm with built-in correction of geometric distortions proposed in this paper allows us to obtain high-quality multi-look SAR images.

References

[1] C. J. Oliver, S. Quegan, Understanding Synthetic Aperture Radar Images. Boston; London: Artech House, 1998.

[2] S. Buckreuss, "Motion errors in an airborne synthetic aperture radar system", European Transactions on Telecommunications, 1991, Vol. 2, No. 6, pp. 655–664.

[3] D. Blacknell et al., "Geometric accuracy in airborne SAR images", IEEE Trans. on Aerospace and Electronic Systems, Mar 1989, Vol. 25, 2, pp. 241-258.

[4] S. N. Madsen, "Estimating the Doppler centroid of SAR data", IEEE Trans. Aerosp. Electron. Syst., vol. 25, pp. 134-140, Mar. 1989.

[5] D. M. Vavriv et al, "Cost-effective Ku-band airborne SAR with Doppler centroid estimation, autofocusing and indication of moving targets", Proc. 2nd European Radar Conf. EuRAD2005, Paris, France, pp. 21-24.

[6] A. Moreira, "Improved Multilook Techniques Applied to SAR and SCANSAR Imagery", IEEE Trans. on Geoscience and Remote Sensing, 29(4), pp. 529-534, July 1991.

[7] O. O. Bezvesilniy, Ie. M. Gorovyi, V. V. Vynogradov, D. M. Vavriv, "Correction of Radiometric Errors by Multi-Look Processing with Extended Number of Looks", Proc. IRS 2010.